X-Rays in Cepheids: Identifying Low-mass Companions of Intermediate-mass Stars

Nancy Remage Evans, Scott Engle, Ignazio Pillitteri, Edward Guinan, H. Moritz Günther, Scott Wolk, Hilding Neilson, Massimo Marengo, Lynn D. Matthews, Sofia Moschou, et al.

The Astrophysical Journal, 938:153 (13pp), 2022 October 20 https://doi.org/10.3847/1538-4357/ac6fdf

X-Rays in Cepheids: Identifying Low-mass Companions of Intermediate-mass Stars*

Nancy Remage Evans[1], Scott Engle[2], Ignazio Pillitteri[3], Edward Guinan[2], H. Moritz Günther[4], Scott Wolk[1], Hilding Neilson[5], Massimo Marengo[6], Lynn D. Matthews[7], Sofia Moschou[1], Jeremy J. Drake[1], Elaine M. Winston[1], Maxwell Moe[8], Pierre Kervella[9], and Louise Breuval[9,10]

[1] Smithsonian Astrophysical Observatory, MS 4, 60 Garden St., Cambridge, MA 02138, USA; nevans@cfa.harvard.edu
[2] Department of Astronomy and Astrophysics, Villanova University, 800 Lancaster Ave., Villanova, PA 19085, USA
[3] INAF-Osservatorio di Palermo, Piazza del Parlamento 1, I-90134 Palermo, Italy
[4] Massachusetts Institute of Technology, Kavli Institute for Astrophysics and Space Research, 77 Massachusetts Ave., NE83-569, Cambridge MA 02139, USA
[5] Department of Astronomy and Astrophysics, University of Toronto, 50 St. George Street, Toronto, ON M5S 3H4 Canada
[6] Department of Physics and Astronomy, Iowa State University, Ames, IA 50011, USA
[7] Massachusetts Institute of Technology, Haystack Observatory, 99 Millstone Rd., Westford, MA 01886, USA
[8] University of Arizona, Steward Observatory, 933 N. Cherry Ave., Tucson, AZ 85721, USA
[9] LESIA, Observatoire de Paris, Université PSL, CNRS, Sorbonne Université, Université de Paris, 5 Place Jules Janssen, F-92195 Meudon, France
[10] Department of Physics and Astronomy, Johns Hopkins University, Baltimore, MD 21218, USA
Received 2022 April 7; revised 2022 May 12; accepted 2022 May 12; published 2022 October 21

Abstract

X-ray observations have been made of a sample of 20 classical Cepheids, including two new observations (Polaris and *l* Car) reported here. The occurrence of X-ray flux around the pulsation cycle is discussed. Three Cepheids are detected (δ Cep, β Dor, and Polaris). X-rays have also been detected from the low-mass F, G, and K companions of four Cepheids (V473 Lyr, R Cru, V659 Cen, and W Sgr) and one hot companion (S Mus). Upper limits on the X-ray flux of the remaining Cepheids provide an estimate that 28% have low-mass companions. This fraction of low-mass companions in intermediate-mass Cepheids is significantly lower than expected from random pairing with the field initial mass function (IMF). Combining the companion fraction from X-rays with that from ultraviolet observations results in a binary/multiple fraction of $57\% \pm 12\%$ for Cepheids with ratios $q > 0.1$ and separations $a > 1$ au. This is a lower limit since M stars are not included. X-ray observations detect less massive companions than other existing studies of intermediate-mass stars. Our measured occurrence rate of unresolved, low-mass companions to Cepheids suggests that intermediate-period binaries derive from a combination of disk and core fragmentation and accretion. This yields a hybrid mass ratio distribution that is skewed toward small values compared to a uniform distribution but is still top-heavy compared to random pairings drawn from the IMF.

Unified Astronomy Thesaurus concepts: Cepheid variable stars (218)

1. Introduction

Massive and intermediate-mass stars typically form as members of a pair or group. This is an important aspect, for instance, of the evolution of angular momentum in the pre-main-sequence phase. Many exotic objects in later phases of evolution arise from the combination of a compact object in a binary or multiple system. For example, this combination produces core-collapse supernovae and even gravitational-wave systems. Cepheids are most commonly approximately $5\,M_{\odot}$ stars, intermediate-mass stars rather than high-mass stars. They typically ultimately become white dwarfs, although the most massive may become neutron stars. However, their binary/multiple characteristics are similar to those of more massive stars and can provide insight into evolution past the main sequence. Cepheid progenitors are B stars. Banyard et al. (2022) provide a recent summary of B-star binary properties for comparison with Cepheid properties.

Components of stars in a multiple system can be challenging to disentangle. Intermediate-mass Cepheids provide good examples of the many approaches needed to derive the masses and separations of the components. Radial velocity studies of spectroscopic binaries (Evans et al. 2015) and high-resolution techniques provide basic information (Evans et al. 2020a), supplemented by proper motions in the Gaia era (Kervella et al. 2019a, 2019b). However, in multiple systems additional information is frequently needed to identify all the system components. For Cepheids, the fact that they have evolved into cool supergiants means that it is possible to identify a complete list of hot companions in ultraviolet spectra (Evans et al. 2013) with spectral types of B and early A (called "late B stars" below). Low-mass companions, however, are more elusive, since the spectrum at ultraviolet, optical, and infrared wavelengths is dominated by the more luminous supergiant. X-rays provide a good remedy for this problem.

Cepheids, like other coronal supergiants (Ayres 2011; Engle 2015), produce a comparatively modest X-ray flux. δ Cep itself typically has an X-ray luminosity $\log L_{\rm X} = 28.6$ erg s^{-1}. However, in an exciting development Engle et al. (2017) found a sharp increase in X-ray flux for a brief period near maximum radius in the pulsation cycle. This was seen in two pulsation cycles and also in the Cepheid β Dor.

Main-sequence stars of spectral types F, G, and K at the age of Cepheids (typically 50 Myr), on the other hand, are much more vigorous producers of X-rays. This makes X-rays a good discriminant between young physical companions of Cepheids and old field stars. Mapping the X-ray production of low-mass main-sequence stars in temperature and age has been an

* Based on observations obtained with the Chandra X-ray Observatory.

important contribution of X-ray studies. We use this legacy to predict X-ray fluxes from possible companions at the age of Cepheids. Details are discussed in Section 4.4.

The vigorous X-ray production of low-mass main-sequence stars adds an important piece to the determination of the properties of the multiple systems of Cepheids and other intermediate-mass stars. X-ray observations of Cepheids where the upper limit is below the level of possible main-sequence companions indicate that a low-mass companion is *not* present. This provides the fraction of Cepheid systems with low-mass companions. Since low-mass stars dominate the stellar mass distribution, identifying them is important for putting together a complete picture of star formation.

A thorough discussion of the observed properties of binary and multiple systems systems is given in Moe & Di Stefano (2017). In particular, they discuss the distributions of mass ratios and separations as a function of mass of the primary and the implications for star formation. The distribution of mass ratios as a function of separation for O and B stars divides into three separation regimes. Close binaries with separations $<$0.4 au favor reasonably massive companions, with $q = M_2/M_1 \simeq 0.5$. In this separation range presumably competitive accretion has resulted in relatively equal masses of the components. Stars in this separation range are not present in the Cepheid sample owing to Roche lobe overflow (RLOF). Systems with wider separations up to 200 au tend to have smaller mass ratios $q \simeq 0.2$–0.3. Companions at wider separations (200–5000 au) in OB systems tend to be outer components in triple systems. Their masses are close to a random pairing with the IMF, favoring low-mass companions. Figure 1 in Moe and Di Stefano shows that the addition of systems with mass ratios q as small as 0.1 in the present study fills a gap for stars as massive as O and B stars. X-rays are the one spectral region where low-mass main-sequence companions can be detected, since at other wavelengths the supergiants outshine dwarfs.

A useful comparison to the fraction of Cepheid plus low-mass systems is the determination of low-mass companions of B and early A stars since these are the stars that evolve into Cepheids. A Chandra observation of the cluster Trumpler 16 (Tr 16) was used to identify X-ray sources among these stars (Evans et al. 2011). Since B and early A stars do not typically produce X-rays, it was assumed that low-mass companions were the X-ray producers. They concluded that 39% of these late B stars have a low-mass companion. Two small points are of note in this comparison. Cepheids are slightly older than Tr 16 B stars, which are $\simeq$3 Myr. In addition, this fraction in Tr 16 includes companions at all separations, where Cepheid binaries with separations smaller than 1 au have been removed owing to RLOF during the red giant phase. However, the Tr 16 results are a good comparison to the Cepheid results in this study.

A second aspect of the present study is that Cepheid upper atmospheres have several properties including X-rays that may bear on outstanding questions. Cepheids frequently have excess infrared (IR) emission from circumstellar envelopes (CSEs) summarized by Gallenne et al. (2021) and Hocdé et al. (2020a, 2020b, 2021). This effect needs to be quantified to allow precise distance determinations using the Cepheid Leavitt (period−luminosity) law in the IR. In addition, the CSEs are related to the long-standing question of possible mass loss in Cepheids. X-ray flux controlled by the pulsation cycle may be a driver of CSEs and hence a clue to understanding both mass loss and the IR Leavitt law.

This study begins with new Chandra observations of two Cepheids (l Car and Polaris) near maximum radius to determine whether they show the flux increase observed in δ Cep. These new data have then been combined with archival data to investigate the occurrence of young low-mass X-ray active companions.

l Car is an important Cepheid because it is bright and also has a long pulsation period (35 days). Long-period Cepheids are vital for determining distances to external galaxies. Like many long-period Cepheids, it has modest variation in some of its parameters, such as its period. This was explored in detail with a combination of radial velocities and interferometry by Anderson et al. (2016).

Polaris is the nearest and brightest Cepheid. An ongoing program is measuring its mass from its astrometric orbit (Evans et al. 2018). The distance to Polaris has been controversial recently. However, the Gaia EDR3 parallax to the resolved companion Polaris B now seems to provide a reliable value of 137 pc (Evans et al. 2018). Polaris has been observed four times in X-rays, once by Chandra (Evans et al. 2011) and three times by XMM-Newton (Engle 2015). All four observations have a reasonably constant X-ray luminosity $\simeq \log L_X = 28.9$ erg s^{-1}. However, none of the observations have been made at the "phase of interest" (maximum radius) for comparison with the X-ray burst of δ Cep. To add to the information about the upper atmosphere, Hubble Space Telescope (HST) COS spectra provide chromospheric emission lines, which have been analyzed by Engle (2015). Polaris also has a radius and CSE measured by interferometry (Merand et al. 2006).

In this paper, subsequent sections discuss observations of l Car and Polaris at maximum radius to search for increased X-ray flux at this phase and the relation of X-ray observations to the pulsation cycle. The sample of X-ray observations of Cepheids is assembled from the new observations, upper limits from the survey investigating resolved companions, and observations where the Cepheids and low-mass companions were detected. This combined sample is compared with X-rays from main-sequence stars. Finally, the discussion includes the fraction of Cepheids in binary and multiple systems and the implications for star formation of these intermediate-mass stars with small mass ratios.

2. Observation and Data Analysis

In order to investigate further the X-ray flux from Cepheids, observations of two stars (l Car and and Polaris) were made with Chandra. The observations were timed exposures with the ACIS-I instrument and are listed in Table 1. Reductions were done with the standard CIAO software package.[11]

l Car.—The long-period Cepheid l Car is known to have period fluctuations like other long-period Cepheids (Anderson 2016; Anderson et al. 2016). The phases of the observations were computed from the period summary in Neilson et al. (2016), including the changing period. The time of observation was selected based on the relation between maximum radius and the burst of X-rays in δ Cep, where the X-ray burst occurs approximately 0.1 in phase after maximum radius. The phase of maximum radius has been measured in three

[11] https://cxc.cfa.harvard.edu/ciao/

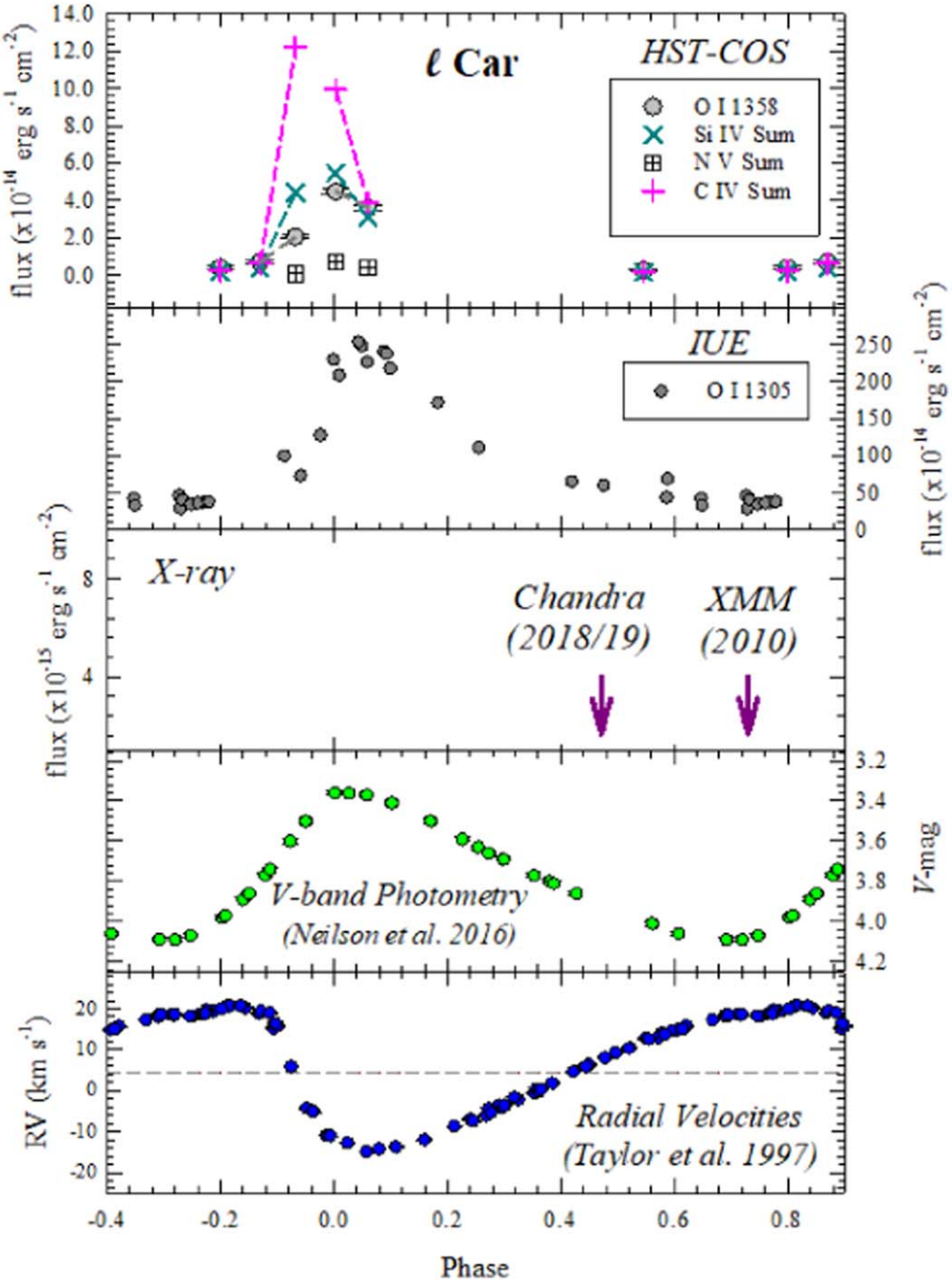

Figure 1. Multiwavelength observations of *l* Car as a function of pulsation phase. Panels top to bottom show emission lines from HST COS spectra, emission lines from IUE spectra, X-ray observations, *V* photometry, and radial velocities as discussed in the text.

Table 1
Chandra Observations

OBSID	Instrument	Exp (ks)	JD (mid)	Phase	D (pc)	log L_X (erg s^{-1})
l Car						
20149	ACIS-I	58.27	2,458,388.9999	0.53	506	<28.26
21858	ACIS-I	20.8	2,458,494.8437	0.51		<28.70
Polaris						
18928	ACIS-I	69.16	2,457,942.1482	0.48–0.59	137	28.83
				0.59–0.69		28.71

successive cycles by Anderson et al. (2016), providing a recent determination of the time of maximum radius. The phase of R_{max} is 0.40, leading to a requested phase of the X-ray observation of 0.50. The phases of observations are listed in Table 1. The observation had to be broken into two parts for scheduling reasons, as listed in Table 1. Note that for a period of 35 days, the duration of the longer exposure covers only 0.02 in phase.

No source was detected at the position of the Cepheid *l* Car. The upper limit to the flux was estimated using $E(B-V) = 0.17$ mag (Fernie et al. 1995), the conversion to N_H from Seward (2000; $N_H/E(B-V) = 5.9 \times 10^{21}$atomscm^{-2} mag^{-1}), and a distance of 506 pc (Evans et al. 2016a). Distances for Cepheids (except Polaris) are taken from Evans et al. (2016a) based on the HST FGS scale of Benedict et al. (2007). Less than 1 count was found for *l* Car in 58.3 ks. Using PIMMS, this provides an unabsorbed flux of 5.88×10^{-16} erg s^{-1} cm^{-2}. At the distance of the Cepheid, this corresponds to a luminosity L_X of 1.75×10^{28} erg s^{-1} (log $L_X = 28.26$). The luminosity upper limit for the short exposure is log $L_x = 28.70$, and that for the combined exposure is log $L_X = 28.11$. Uncertainties on the upper limits are based on the variance of the background. For *l* Car, the exposure time (corrected to 44 ks of good time intervals) corresponds to a 9% uncertainty, or a difference of 0.04 in log L_X.

Polaris.—For Polaris, similarly, the observation was requested to coincide with the predicted time of X-ray increase shortly after maximum radius. Phases of observation were computed from the recent ephemeris (Engle 2015): 2,455,909.910+3.972433 E. The phase range covered by the observation is 0.48−0.69.

A source was detected at the position of Polaris. A flux was determined by fitting the spectrum with a MEKAL model in CIAO with $E(B-V) = 0.00$ and a fixed temperature of 0.56 keV, typical of a young star. MEKAL models were used for consistency with data from Engle (2015); however, tests with newer APEC models agreed to 10%. The resulting flux is 2.08×10^{-14} erg s^{-1} cm^{-2}. The distance used to determine the luminosity is 137 pc from the Gaia EDR3 distance to the resolved companion Polaris B. Because of the length of the exposure, the luminosity was computed for two halves, log L_X = 28.83 and 28.71 [erg s^{-1}]. The details are listed in Table 1.

3. The Pulsation Cycle

The interest in X-ray production in Cepheids is enhanced by its relation to other parameters of the pulsation cycle. In the case of δ Cep (Engle et al. 2017), a brief X-ray burst was seen shortly after *maximum* radius. This is in contrast to ultraviolet chromospheric lines, which go into emission after *minimum* radius.

l Car.—The relation of the X-ray observations in Table 1 to other pulsation parameters is shown in Figure 1, adapted from Neilson et al. (2016). Successive panels show emission lines from HST COS spectra and from International Ultraviolet Explorer (IUE) spectra, upper limits from Chandra (Table 1) and XMM-Newton observations, *V*-band photometry (Neilson et al. 2016), and radial velocities (Taylor et al. 1997).

Polaris.—The relation of the X-ray observations of Polaris to the pulsation cycle variables is shown in Figure 2. Successive panels show N V and Si IV emission lines from HST COS spectra (Engle 2015), X-ray observations, *V*-band photometry (Engle 2015; plus some additional data from the same system), and radial velocities (Anderson 2019). Four previous observations with XMM-Newton and Chandra are listed in Engle (2015).

4. X-ray Observations of Cepheids

In addition to the observations of *l* Car and Polaris, X-ray observations have been made of a number of Cepheids. δ Cep, β Dor, *l* Car, and SU Cas are discussed in Engle (2015). Observations of V473 Lyr and η Aql are discussed in Evans et al. 2020b, 2021), respectively. Finally, a survey was made with XMM-Newton of possible resolved companions (Evans et al. 2016b). In this section we discuss these observations in three subsections: upper limits in cases where the Cepheid was not detected (Table 2), cases where the Cepheid was detected (Table 3), and cases where a low-mass companion was detected (Table 4).

4.1. Upper Limits for Cepheids and Close Companions

A series of observations were conducted with XMM-Newton of Cepheids with possible resolved low-mass companions (Evans et al. 2016b). The resolved companion candidates are separated from the Cepheids typically by 10″; hence, these observations also provide an X-ray observation of the Cepheid and any possible close companion as well. For the resolved companions, because low-mass stars at the age of Cepheids are X-ray active, they can be distinguished from old line-of-sight field stars in X-ray observations. The companion candidates in the XMM-Newton survey were identified in an HST Wide Field Camera 3 (WFC3) snapshot survey. The exposure time was set to detect a late spectral type companion (see Section 4.4). Because young low-mass main-sequence stars are more X-ray active than supergiant Cepheids, in general the observations of the Cepheids themselves are upper limits. They are summarized in Table 2. Columns in Table 2 list the star, the satellite used, the epoch and period used to compute the phase where they are not provided in another source, the reference for the period, the JD of mid-exposure where it is not listed elsewhere, the pulsation phase of the observation, the distance *D* from Evans et al. (2016a), and the log of the X-ray luminosity of the upper limit. The distances are on the Benedict et al. (2007) scale. Where the observations covered a significant range of phases, the range is shown. For most observations, the exposure time only covered ±0.03 in phase. The upper limits are based on a 3σ detection since the positions of the sources are known, as discussed in Evans et al. (2016b). Uncertainties for the upper limits were estimated from the standard deviation of the local background. As a typical example, V440 Per has an exposure time of 21 ks and an uncertainty on the upper limit of 9%, corresponding to 0.04 in log L_X.

The upper limits to Cepheid X-rays are plotted in Figure 3.

In addition, upper limits to two Cepheids (SU Cas and *l* Car) were reported by Engle (2015) from XMM-Newton observations, which are listed in Table 2. Neither was detected. For the short-period Cepheid SU Cas ($P = 1.95$ days), the upper limit log $L_X = 29.46$ erg s^{-1} was estimated using exposure times and background rates and a distance $D = 376$ pc. For *l* Car the upper limit was estimated using a distance 506 pc to be log $L_X = 29.62$ erg s^{-1}.

η Aql was also observed by XMM-Newton (Evans et al. 2021) but not detected (Table 2), providing an upper limit.

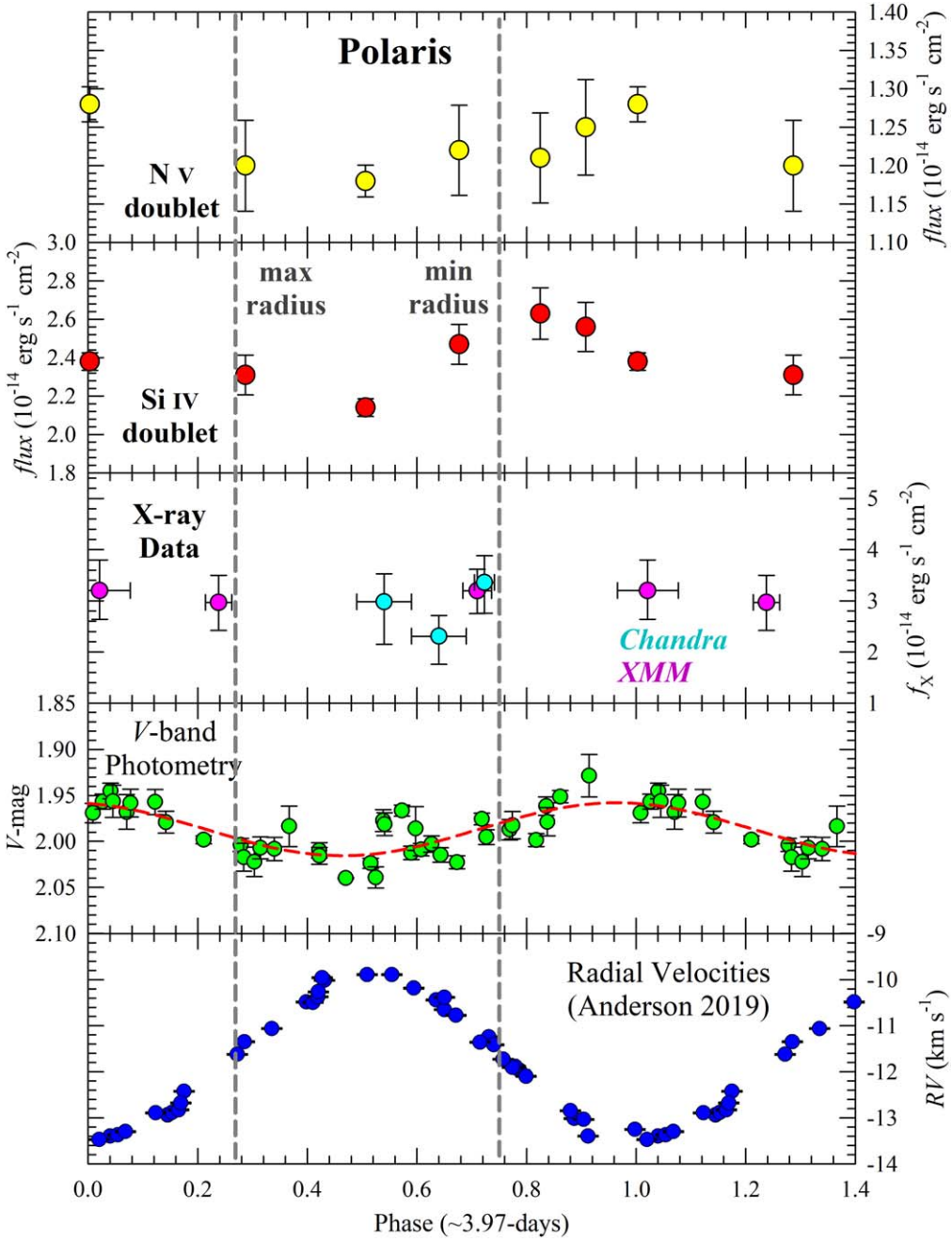

Figure 2. Multiwavelength observations of Polaris as a function of pulsation phase. Panels top to bottom show N V emission lines and Si IV emission lines from HST COS spectra, X-ray observations, *V* photometry, and radial velocities as discussed in the text. The error bars on the X-ray phases indicate the time period covered by the observations. The Chandra observation in Table 1 has been broken into two parts.

4.2. Detections of Cepheids

For the Cepheids δ Cep, β Dor, and Polaris the Cepheid itself was detected (Engle 2015). The observations are listed in Table 3 and are shown in Figure 3.

There is some evidence for a low-mass companion to δ Cep from radial velocities (Anderson et al. 2015), interferometry (Gallenne et al. 2016), and Gaia (Kervella et al. 2019b). While this is possible, Figure 3 shows that the X-ray level is lower than any main-sequence star hotter than spectral type M.

In the 10-day Cepheid β Dor a variation in luminosity is seen, with the largest value at about the same level as the maximum luminosity of δ Cep. The 10-day Cepheids fall in the Hertzsprung progression of light curves, where the pulsation amplitude is decreased by the coincidence of the primary and secondary humps. This may distort the phase of maximum light, which is the standard ephemeris fiducial. We have determined the phase of the X-ray increase in β Dor as follows. For δ Cep (Figure 1 in Engle et al. 2017) both the phases when the pulsation wave passes through the photosphere at minimum radius and the phase of X-ray maximum shortly after maximum radius are well determined from far-UV (FUV) lines and X-ray fluxes, respectively. The X-ray flux maximum occurs 0.66 phase after the FUV flux maximum. Similarly, the phase of FUV maximum (minimum radius) of the photospheric pulsation wave is well determined for β Dor. If we match the phases of UV maximum in δ Cep and β Dor (by adding 0.17 to

Table 2
X-ray Upper Limits of Cepheids

	Sat	T_0 (−2,400,000)	P (days)	Reference	JD mid (−2,400,000)	Phase	D (pc)	log L_X (erg s^{-1})
η Aql	XMM	55,856.689	7.177025	1	58,616.02	0.41–0.53	273	<29.23
l Car	Chan	37,751.5	35.535	2	58,389.00	0.55	506	<28.26
l Car	Chan			2	58,494.84	0.52	506	<28.70
l Car	XMM			3	55,232.31	0.76	506	<29.62
SU Cas	XMM	55,199.614	1.949330	3	55,236.27	0.64–0.98	376	<29.46
V737 Cen	XMM	55,118.3272	7.0659	4	56,684.28	0.62	848	<29.40
S Cru	XMM	34,973.495	4.689970	5	56,525.48	0.34	724	<29.60
X Cyg	XMM	43,830.251	16.385692	6	56,408.79	0.65	981	<29.89
R Mus	XMM	26,496.033	7.510159	5	56,338.66	0.63	844	<29.48
S Nor	XMM	44,018.884	9.754244	5	57,095.07	0.56	910	<29.44
Y Oph	XMM	39,853.173	17.126908	5	56,182.84	0.45	510	<29.29
V440 Per	XMM	44,551.137	7.572498	6	56,538.55	0.02	791	<29.17
U Sgr	XMM	30,117.955	6.745229	5	54,020.65	0.64	617	<29.05
Y Sgr	XMM	40,762.329	5.773380	5	56,564.79	0.12	505	<29.25

Note.
Period source: (1) Evans et al. 2021; (2) Table 1; (3) Engle 2015; (4) Usenko et al. 2013; (5) Szabados 1989; (6) Szabados 1991.

Table 3
X-Ray Detections of Cepheids

	Sat	Reference	Phase	D (pc)	log L_X (erg s^{-1})
Polaris	XMM	1	0.21–0.26	137	28.82
Polaris	XMM	1	0.68–0.74	137	28.86
Polaris	XMM	1	0.97–0.08	137	28.90
Polaris	Chan	1	0.71–0.73	137	28.88
Polaris	Chan	2	0.48–0.59	137	28.83
		2	0.59–0.69	137	28.71
δ Cep	XMM	3	0.33–0.39	255	28.60
	XMM	3	0.43−0.48	255	29.17
	XMM	3	0.48−0.54	255	28.90
	XMM	3	0.54−0.59	255	28.66
	XMM	3	0.05−0.12	255	28.67
	XMM	3	0.84−0.96	255	28.53
	XMM	3	0.96−0.08	255	28.53
	XMM	3	0.58−0.68	255	28.46
	XMM	3	0.68−0.78	255	28.66
	Chan	3	0.48−0.52	255	29.16
	Chan	3	0.52−0.56	255	28.95
β Dor	XMM	1	0.58–0.62[a]	335	29.24
β Dor	XMM	1	0.64–0.68[a]	335	29.11
β Dor	XMM	1	0.69–0.73[a]	335	28.94

Notes.
Sources: (1) Engle 2015; (2) Table 1; (3) Engle et al. 2017.
[a] Phases adjusted; see text.

the phase of UV maximum in β Dor), the phase of X-ray maximum becomes 0.42, as shown in Figure 3, very similar to the phase of δ Cep. This phase adjustment is included in the β Dor phases in Table 3.

4.3. Detections of Cepheid Companions

In some cases X-ray observations identified low-mass companions of Cepheids. Each of those will be discussed in this section. They are summarized in Table 4 and Figure 3.

V473 Lyr.—This is a unique Cepheid with a variable amplitude, perhaps similar to the Blazhko effect in RR Lyrae stars. A recent XMM-Newton observation (Evans et al. 2020b) was made to follow up a possible X-ray burst. However, the X-ray flux remained constant for a third of the pulsation cycle, making a low-mass companion the most likely interpretation. Limits from radial velocities and Gaia proper motions are consistent with a companion at a separation between 30 and 300 au.

V659 Cen.—The Cepheid is in a multiple system, and its components are only identified using a number of approaches. A resolved companion at 0.″6 (452 au) was found in an HST WFC3 survey of Cepheids (Evans et al. 2013). The system was found to be an X-ray source in the XMM-Newton survey of possible resolved companions (Evans et al. 2016b) with log $L_X = 29.51$ erg s^{-1} at a pulsation phase of 0.14. In the summary discussion of the HST WFC3 survey, Evans et al. (2020a) found that systems with a resolved companion also have an inner spectroscopic binary. Evidence for an inner binary in the V659 Cen system discussed there includes orbital motion in velocities and possible orbital motion in Hipparcos proper motions. Can we identify the source of the X-rays in the triple system? In comparison with Cepheids, which have themselves been detected in X-rays (Table 3), V659 Cen has a much larger X-ray flux, particularly at the phase of the observation. V659 Cen B, the hottest star, has a spectral type of B6 V from the ultraviolet spectrum (Evans et al. 2020a). The same study discusses an HST STIS ultraviolet spectrum oriented to resolve the Cepheid and the 0.″6 companion, which shows that the hottest star in the system is the resolved companion V659 Cen B. Could the X-rays be produced by that star? X-rays are produced by O and early B stars (Berghoefer et al. 1997; Naze et al. 2011). However, the dividing line for X-ray producers is approximately B3 V. V659 Cen B is cooler than that and unlikely to produce X-rays. The spectroscopic binary companion V659 Cen Ab is a lower-mass star and hence should be able to produce X-rays, and, indeed, the X-ray flux is reasonable for an F, G, or K star. The components are summarized in Figure 4(a).

R Cru.—X-ray flux from the R Cru system was discovered by Evans et al. (2016b) in an XMM-Newton survey of possible resolved companions. The HST observations showed two possible companions as sources of the X-rays, one at 1.″9 and a closer spectroscopic binary. A shallower Chandra exposure

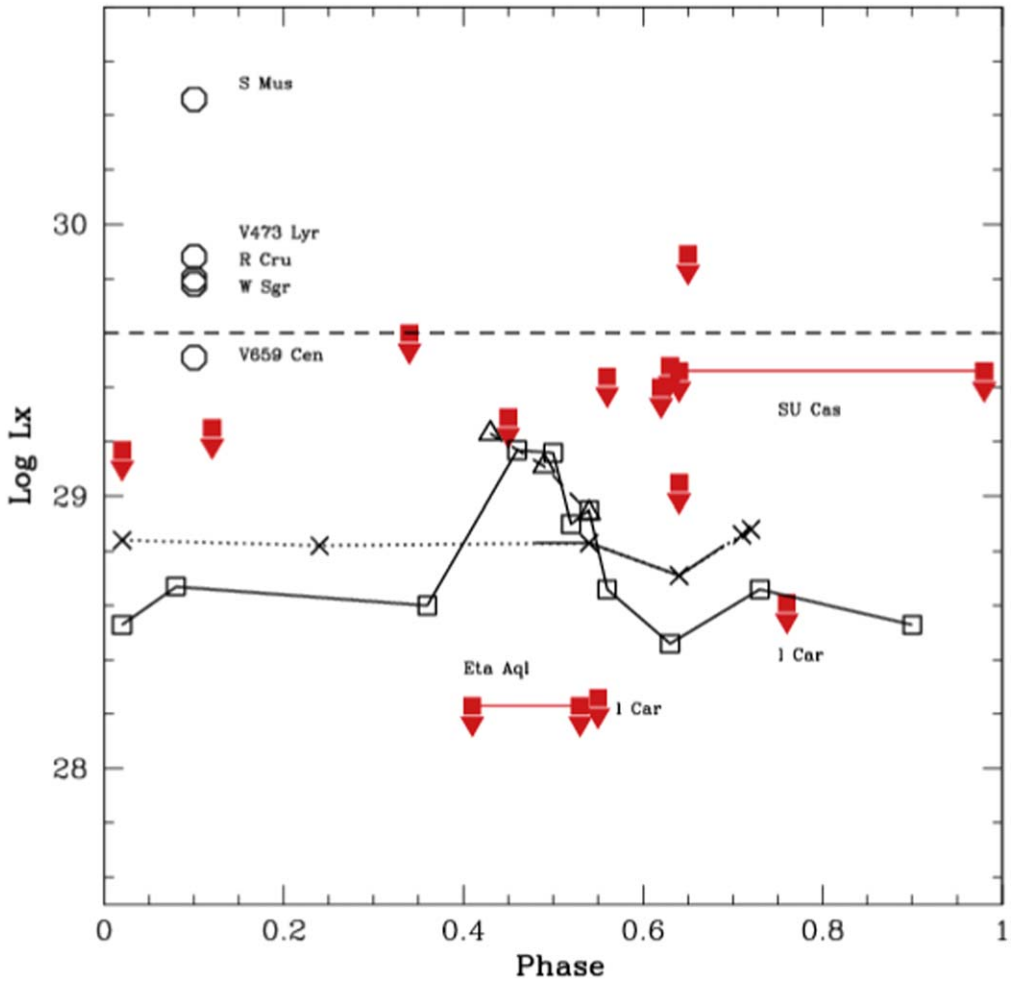

Figure 3. X-ray observations of Cepheids. Upper limits from nondetections in Table 2 are filled red downward-pointing arrows. Detections of Cepheids in Table 3 are as follows: δ Cep (connected open squares), Polaris (connected crosses), and β Dor (connected triangles). The solid portion of the Polaris data line shows the phase range of the new observation in Table 1. For η Aql and SU Cas upper limits are indicated and the lines show the phase range covered. The mean log L_X for F, G, and K main-sequence stars is shown by the dashed line at log $L_X = 29.6$. Circles in the upper left corner (labeled) are systems where the low-mass companion dominates the X-rays (Table 4). Luminosity is in erg s^{-1}.

Table 4
X-Ray Detections of Cepheid Companions

	Sat	T_0 (−2,400,000)	P (days)	Reference P	JD mid (−2,400,000)	Phase	D (pc)	log L_X (erg s^{-1})
V473 Lyr	XMM	[a]	1.490813	1	56,557.96	0.47	553	29.88
	XMM			1	58,560.00	0.42-0.73		30.07
S Mus	XMM	40,299.163	9.659875	2	56,298.26	0.24	789	30.46
W Sgr	XMM	43,374.622	7.594904	2	57,637.64	0.97	409	29.78
	XMM				57,659.39	0.83		
V659 Cen	XMM	52,358.9089	5.62316689	3	56,543.46	0.14	753	29.51
R Cru	XMM	55,172.5100	5.825701	4	56,662.46	0.73	829	29.80

Notes.
Sources: (1) Evans et al. 2020b; (2) Szabados 1989; (3) Berdnikov et al. 2000; (4) Usenko et al. 2014.
[a] The phase for V473 Lyr very variable.

localized the X-rays to the spectroscopic binary companion (Evans et al. 2020a). (Removal of the 1.″9 companion also removes the most discordant point in the color–magnitude diagram of companions in Figure 6 in Evans et al. 2020a.) In addition, there is a star at 7.″7 (Evans et al. 2020a; Kervella et al. 2019b). It was considered a likely companion from Gaia DR2 data. However, in the EDR3 data, both the parallax and the proper motion do not match those of the Cepheid as closely, and they are less likely to be physically related. The system thus contains a Cepheid R Cru Aa and the likely spectroscopic binary companion R Cru Ab (Evans et al. 2020a). The X-ray luminosity in Table 4 is from the deeper XMM-Newton observation.

S Mus.—X-rays were similarly discovered in the S Mus system in the XMM-Newton observation by Evans et al. (2016b),

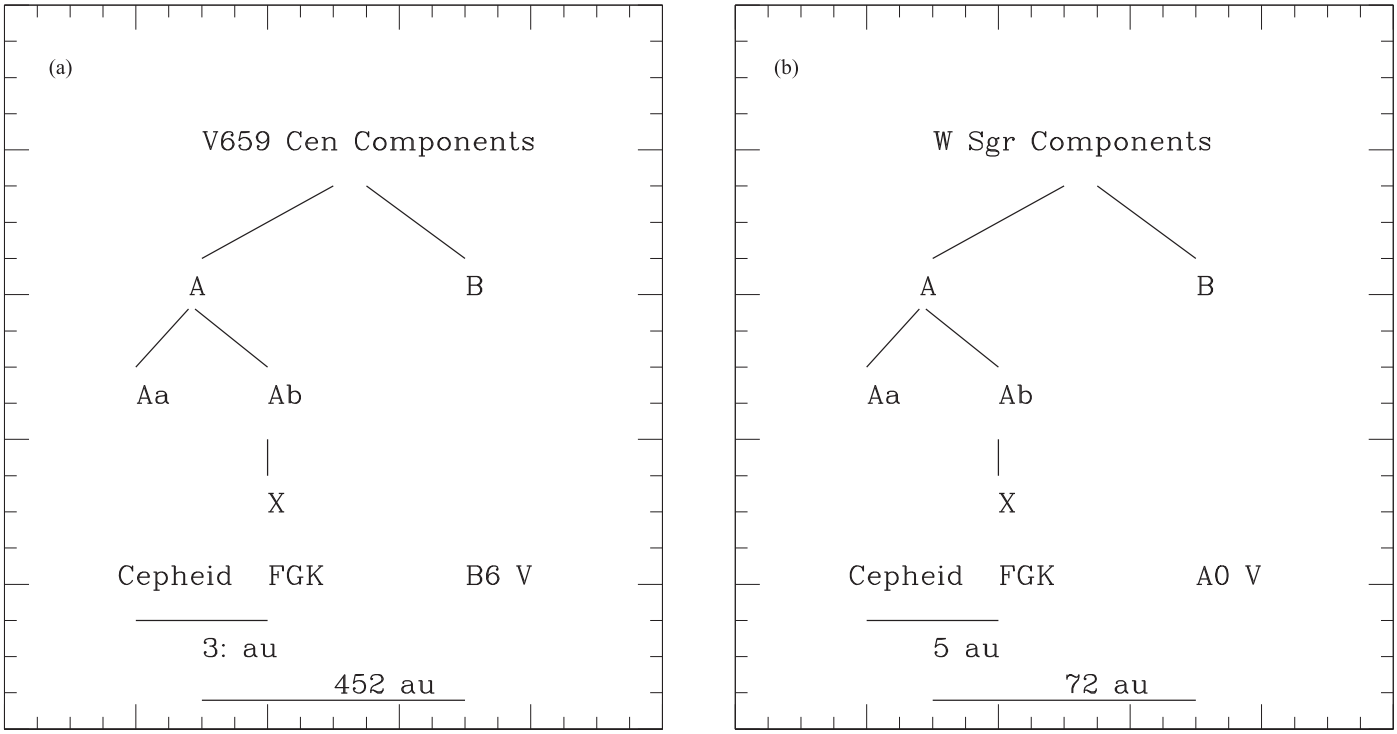

Figure 4. (a) The V659 Cen system. The diagram of the components indicates the Cepheid and the spectral types of the close and distant binary. Star Ab is a low-mass star (FGK) that produces the X-rays. The separations of the systems in au are indicated at the bottom. (The separation in the Aa–Ab binary is only an estimate.) (b) The W Sgr system, with the same notation as in panel (a).

which was followed by a Chandra observation to localize the X-rays (Evans et al. 2020a). In this case, the X-rays come from a spectroscopic binary with a period of 505 days made up of the Cepheid and a B3 V companion. A companion this hot can produce X-rays through wind shocks, so the most likely interpretation is that the hot companion is responsible for the X-rays. S Mus is thus the one Cepheid that is not an X-ray test for a low-mass companion. The X-ray luminosity in Table 4 is from the XMM-Newton observation.

W Sgr.—X-ray flux was found at the location of the Cepheid by XMM-Newton, listed in the source catalog 4XMM-DR11.[12] There are in fact two XMM-Newton observations of W Sgr. In the second, the star is at the border of a chip; hence, the flux is less precise. The stacked observation has a flux of $(3.0 \pm 0.4) \times 10^{-14}$ erg s^{-1} cm^{-2} in 0.2–12 keV. This is log $L_X = 29.78$ at 409 pc.

W Sgr is part of a triple system (Evans et al. 2009). The hottest companion to the Cepheid, W Sgr B, has spectral type A0 V (Evans et al. 2013) and was resolved from the spectroscopic binary in an HST STIS spectrum (Evans et al. 2009) at a projected distance of 72 au. The spectroscopic binary Aa + Ab has separation of 5.0 au (Benedict et al. 2007). Only an upper limit could be obtained for the mass and spectral type of the companion from the STIS spectrum ($<1.4\,M_\odot$ and later than F5 V). This is consistent with the X-ray luminosity. Components are summarized in Figure 4(b).

4.4. X-rays from Main-sequence Stars

Studies of activity in main-sequence stars have been a very important area of X-ray study. The X-ray luminosities in the sequence of open clusters of different ages are summarized, for instance, in Prebisch & Feigelson (2005). The age of stars found in the instability strip depends on their mass and hence their pulsation period. A typical age is 50 Myr as discussed by Bono et al. (2005). This is between the ages of the Orion Nebula Cluster and the Pleiades, with the α Per cluster being a good representation of stars of this age. Its age is estimated to be from 50 Myr (Meynet et al. 1993) to 90 Myr (Stauffer et al. 1999). A study was made by Randich et al. (1996) of ROSAT observations of the full cluster found that at a depth of log L_X of 29.5 erg s^{-1}, 76% and 79% of G and K stars were detected, respectively. Even for F stars, 75% were detected, although early F stars are not strong X-ray producers. A more recent study of a deep XMM-Newton observation of the α Per cluster is presented by Pillitteri et al. (2013). They find a mean X-ray luminosity log L_X of 29.63 erg s^{-1} for F main-sequence stars, 29.74 erg s^{-1} for G dwarfs, and 29.56 erg s^{-1} for K dwarfs. M dwarfs are fainter and are not expected to be detected in the present study. A line is included at 29.6 erg s^{-1} in Figure 3 to indicate the mean level of F, G, and K stars. There are, of course, a range of X-ray luminosities for any mass or spectral type. This is partly because of variation of rotation velocity between stars. In addition, cool stars have activity cycles. However, even at a depth of log $L_X = 29.5$, Randich et al. find that they detect three-quarters of F, G, and K stars or better.

5. Low-mass Companions of Cepheids

A sample of 20 Cepheids observed in X-rays has been assembled from observations made for a variety of purposes. The X-ray luminosity level has been established for quiescent phases from δ Cep and Polaris at log $L_X \simeq 28.7$ erg s^{-1}. On the other hand, deeper exposures for l Car and η Aql have not detected the Cepheid at log $L_X = 28.2$ erg s^{-1}.

[12] http://xmm-catalog.irap.omp.eu/sources

Table 5
Mass/Spectral Type Regions for Companion Detection

	Sp Ty UV Hot		Sp Ty UV Cool		Sp Ty X Hot		Sp Ty X Cool		
Bin		1		2		3		4	
Spectral type	B5		A5		F5		M0		M5
Mass ($M_{\odot}$)	5.9		1.9		1.4		0.51		0.21
Mass ratio		3.1		1.4		2.8		2.4	
Companion (%)		21		…		28		…	

For the Cepheids W Sgr, V473 Lyr, V659 Cen, and R Cru a young low-mass companion dominates the X-ray range. For S Mus the X-ray flux is most likely produced by an early B hot companion, which reduces the sample to 19 Cepheids to look for low-mass companions. For the remaining 15 Cepheids, the upper limits indicate that there is *not* a low-mass companion. Thus, only 21% of the Cepheids clearly have a low-mass companion. This fraction would be increased slightly if two stars with upper limits above or on the dividing line were removed from the sample. The sample has some limitations. Systems with periods shorter than a year are not present in Cepheid samples because they would have disappeared owing to RLOF, particularly at the tip of the red giant branch. The X-ray exposure depth was set to detect F, G, and K main-sequence stars at the age of the Cepheids. Thus, M companions would not have been detected. In X-ray studies of main-sequence stars at this age, three-quarters of F, G, and K companions would have been detected at this exposure depth. This correction would raise the fraction of systems with low-mass companions to 28^{+13}_{-9}% (errors from binomial statistics). This is clearly much lower than a random selection of companions from the IMF (Chabrier 2003; Moe & Di Stefano 2017), at least for systems with separations greater than about 1 au.

6. Discussion

6.1. Binary/Multiple Fraction of Cepheids

All methods of identifying Cepheid companions have some limitations. The X-ray observations in the current paper do not detect companions of spectral types earlier than F or later than K. However, they identify companions at any separation. Similar properties are true for UV surveys: they identify companions earlier than mid-A at any separation (Evans et al. 2013). Radial velocities (Evans et al. 2015) and Gaia proper motions (Kervella et al. 2019a), on the other hand, are sensitive to a wider range of spectral types but detect short-period, small-separation systems, but not longer-period systems. Velocity studies are also much more sensitive for sharp-lined stars such as Cepheids than for broad-lined hot stars.

Ultimately, results for X-ray studies and ultraviolet studies of Cepheids need to be combined into the binary/multiple star fraction. The X-ray fraction (28%) and the UV fraction (21%; Evans 1992) are comprehensive for the companion spectral types they cover. However, Cepheids, like other intermediate-mass and massive stars, are frequently found in systems with more than two members, and thus results from these two "detection wavelength" approaches would sometimes overlap. We can make a rough estimate of this from this study, in that of the four Cepheids with a late-type companion, two (V659 Cen and W Sgr) were already known to be in multiple systems from UV studies. That is, only half of the low-mass companions (14%) are new systems in the total, resulting in 35% of Cepheids in binary or multiple systems from the combined X-ray and UV studies. This is, of course, a lower limit since it does not represent all companion spectral types. We can further make rough estimates of the companions that are left out of these two spectral type regions. The UV spectra identify all massive companions but have serious incompleteness starting at mid-A spectral types, corresponding to a mass of approximately 1.9 $M_{\odot}$. Table 5 summarizes information about these spectral type regions (bins). The top row lists the spectral types of the hot and cool boundaries of the UV and X-ray surveys. Corresponding masses are listed in the next line taken from Drilling & Landolt (2000). Below the masses, the entries list information for the four bins. The mass ratio is shown for the mass range in the bin. The bottom line shows the percentage of companions measured in bins 1 and 3. The mass ratios in line 3 are quite similar for the X-ray and UV regions and also for the regions not covered. Following the results from the IMF (Chabrier 2003), the region in bin 2 not sampled in X-ray or UV is expected to have somewhat fewer stars than the sampled regions and hence fewer binary companions. Thus, the missing region in bin 2 would probably not double either the fraction in bins 1 and 3 or the combined fraction (35%), but it would add significantly. Similarly, the missing M stars in bin 4 would substantially increase the fraction. However, we have shown here that the fraction of cool companions in binary systems is less than predicted by a field IMF. In sum, the binary fractions in bins 1, 2, and 3 are 21%, <21%, and 28%, respectively. A simple total is <70%. It would be reduced somewhat by an overlap of UV and X-ray companions in multiple systems. However, it would be increased by a substantial but unknown fraction of M stars in bin 4.

The second binary/multiple detection technique is through orbital motion, either with radial velocities or with proper motions. Evans et al. (2015) examine orbital motions for the 40 brightest Cepheids north of −20° from two CORAVEL studies. They find a binary fraction of 29% with orbital periods between 1 and 20 yr where the sample is most complete. This rises to 35% for all periods greater than 1 yr for the nearest 40 stars. There is serious incompleteness for long orbital periods and low mass ratios. Since, from this X-ray study, companions F5 V or cooler are likely to be at least half the binary fraction, the incompleteness rises substantially. Kervella et al. (2019a) have compared Gaia DR2 proper motions with those from Hipparcos to identify deviations resulting from orbital motion (proper motion anomalies). Using their criterion for a detection of the ratio of proper-motion difference to signal-to-noise ratio of 3, for the nearest 100 Cepheids, the binary fraction is 32%. This fraction doubles adding in binaries identified by other means, bringing it close to the estimate of 70% above.

Wider companions in orbits that would not be identified from either velocities or proper motions also exist. The challenge here is that as larger separations from the Cepheid are searched, a field star is more likely to be included in the list

of companion candidates. This was tested with X-ray observations of a subset of possible resolved companions (Evans et al. 2016b). No companion candidates with separations >5″ or 4000 au were confirmed to be physical companions. There are six systems with wider companions or possible companions in the HST survey (Evans et al. 2020a), but most have a hot companion or are in spectroscopic binary systems, so they are already counted and do not add to the list of binary or multiple systems. Gaia DR2 and EDR3 parallaxes and proper motions have also been used to investigate companions at wider separations (Kervella et al. 2019b; Breuval 2021). This is a very promising approach, but so far for the Cepheids within about 1 kpc, the companion candidates all have sizable errors in EDR3 parallaxes.

The most important feature in comparing the Cepheid binary fraction with that of B stars from which Cepheids evolved is RLOF for short-period B binaries. The effects are particularly striking in O stars (Sana et al. 2012). Moe & Di Stefano (2017) find that only 75% of mid-B stars will evolve into Cepheids. This means that our fraction of Cepheids with low-mass companions (28%; Table 5) corresponds to a fraction of 37% of B stars.

The fraction of low-mass companions of Cepheids can be compared with that of "late B" stars in Tr 16 (39%) from a similar X-ray technique (Evans et al. 2011). This is very close to the Cepheid fraction (37%). The fraction in Tr 16 might be somewhat higher since the cluster is younger than the Cepheids, and hence low-mass stars are more X-ray active and more easily detected. Furthermore, the Cepheid sample is limited to binaries with periods longer than a year. However, the similarity of the fractions indicates that in both the occurrence of low-mass companions is lower than would be predicted by random sampling from a field IMF.

6.2. Implications for Star Formation

Unresolved companions to Cepheids provide a unique probe into the properties of intermediate-mass binaries across intermediate separations, which helps to constrain binary formation models. The unresolved companions must be wider than $a > 1$ au to avoid RLOF with the Cepheid supergiant primaries, and they must also reside within $a < 1000$ au; otherwise, we would have resolved the companions in our previous HST imaging campaign (Evans et al. 2020a). Our detected X-ray companions span late F/G/K dwarfs, corresponding to masses $M_{\rm comp} = 0.5$–$1.4\,M_{\odot}$. For a typical Cepheid primary mass of $M_{\rm Cepheid} \approx 5\,M_{\odot}$, the binaries correspond to mass ratios $q = M_{\rm comp}\ /M_{\rm Cepheid} = 0.10$–$0.28$. After correcting for incompleteness of FGK stars that do not produce a detectable X-ray flux as described above, we conclude that 28^{+13}_{-9}% of Cepheids have companions across $a = 1$–1000 au and $q = 0.10$–0.28 (red data point in Figure 5), where the uncertainties derive from binomial statistics. For a larger sample of 76 Cepheids, 16 exhibited a UV excess from unresolved B/early A dwarfs spanning $M_{\rm comp} = 1.9$–$5.9\,M_{\odot}$ (Evans 1992). We thus find that $21\% \pm 5\%$ of Cepheids have companions across $a = 1$–1000 au and $q = 0.37$–1.00 (magenta data point in Figure 5). We are incomplete to late A/early F dwarf companions, which span the narrow mass ratio interval $q = 0.28$–0.37.

As shown in Figure 5, companions to Cepheids are skewed toward smaller mass ratios. Given the measured occurrence rate of B/late A companions to Cepheids via the UV excess method and assuming a uniform mass ratio distribution (dotted line in Figure 5), we would have expected only 6% of Cepheids to have late F/G/K companions across $q = 0.10$–0.28. This prediction is discrepant with our empirical measurement of 28^{+13}_{-9}% at the 2.7σ level. Conversely, if we instead assumed that binaries were drawn from random pairings of the IMF (dashed curve in Figure 5), we would have expected 87% of Cepheids to have companions across $q = 0.10 - 0.28$, which is even more inconsistent with our measurement at the 4.5σ level. The true mass ratio distribution is between these two slopes. By fitting a single power-law distribution $p_q \propto q^{\gamma}$, we measure $\gamma = -1.2 \pm 0.4$ across $q = 0.11.0$ (blue curve in Figure 5).

Close companions ($a < 1$ au) to mid-B stars follow a uniform mass ratio distribution, indicating that they coevolved via shared accretion in a circumbinary disk, while wide companions ($a > 1000$ au) are weighted toward extremely small mass ratios, nearly consistent with random pairings drawn from the IMF, suggesting that the components fragmented and subsequently accreted fairly independently (Abt et al. 1990; Kobulnicky & Fryer 2007; Kouwenhoven et al. 2007; Moe & Di Stefano 2017). Across intermediate separations, both long-baseline interferometry (Rizzuto et al. 2013) and decomposition of binaries from high-resolution spectra (Gullikson et al. 2016) demonstrated that the mass ratio distribution is skewed toward small mass ratios. However, these techniques are insensitive to companions below $q < 0.3$. Our survey yields the first robust census of low-mass companions to intermediate-mass stars across intermediate separations, confirming earlier indications that the mass ratio distribution is skewed toward small mass ratios but nonetheless still top-heavy compared to random pairings drawn from the IMF. Thus, both disk and core fragmentation and accretion lead to a mixed population of intermediate-period binaries.

Moe & Di Stefano (2017) adopted a segmented power-law mass ratio distribution, with the parameter $\gamma_{\rm largeq}$ describing the slope across large mass ratios $q = 0.3$–1.0 and $\gamma_{\rm smallq}$ across $q = 0.1$–0.3. They fitted both power-law slopes as a function of primary mass and orbital separation based on a combination of data sets, interpolating over the gaps in the observations. For intermediate-period companions to $5\,M_{\odot}$ primaries, they fitted $\gamma_{\rm largeq} = -2.0$ and $\gamma_{\rm smallq} = 0.0$ (green curve in Figure 5). This distribution is significantly skewed toward small mass ratios, nearly consistent with random pairings of the IMF across $q = 0.3$–1.0, but then flattens to a uniform distribution below $q < 0.3$. Their broken power-law model is also consistent with our measurements.

We can now determine the overall unresolved binary fraction of Cepheids. By interpolating our best-fit power-law model across the mass ratio gap where both X-ray and UV methods are insensitive, we expect an additional 8% of Cepheids to have late A/early F companions across $q = 0.28$–0.37. Thus, $57\% \pm 12\%$ of Cepheids have companions across $q = 0.1$–1.0 and $a = 1$–1000 au. This is consistent with expectations from mid-B binaries. Moe & Di Stefano (2017) estimated that 85% of $5\,M_{\odot}$ main-sequence primaries have companions above $q > 0.1$, of which 70% have intermediate separations spanning $a = 1$–1000 au. Hence, $0.85 \times 0.70 = 60\%$ of mid-B stars have companions across intermediate separations, nearly identical to our Cepheid result.

The X-ray studies here demonstrate that the fraction of F, G, and K companions is smaller than would be produced by random pairings of the IMF (Figure 5). To complete the understanding of companion distribution, we need to know the form of the distribution of M-star companions. A recent study of b Cen, a 6–$10\,M_{\odot}$ binary, demonstrates that even a planet

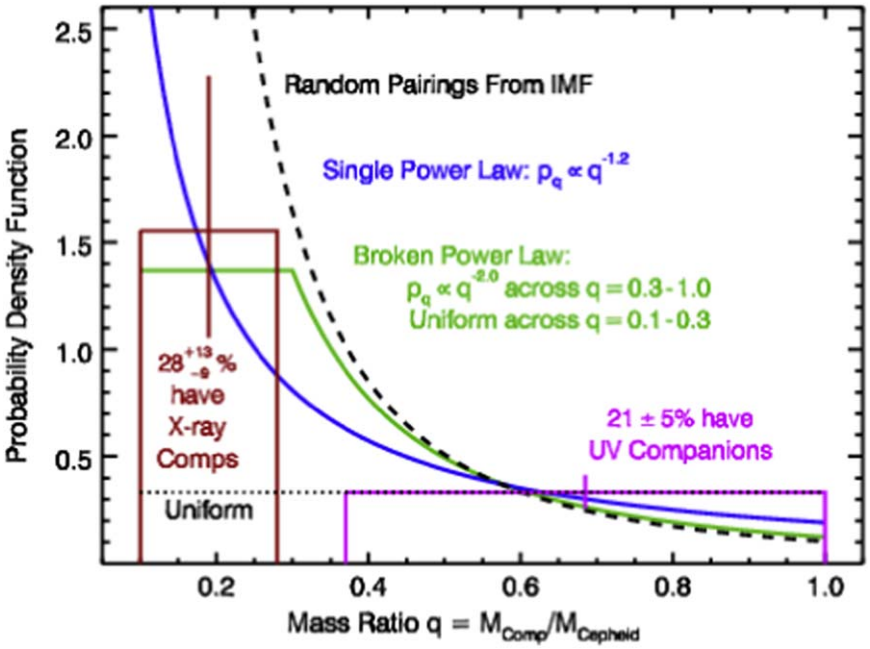

Figure 5. Our X-ray survey demonstrates that $28^{+13}_{-9}\%$ of Cepheids have unresolved late F/G/K companions across $q = 0.10$–0.28 (red). Meanwhile, an earlier UV survey (Evans 1992) found that $21\% \pm 5\%$ of Cepheids have unresolved B/early A companions across $q = 0.37$–1.0 (magenta). The measured mass ratio distribution is inconsistent with both a uniform distribution (dotted) and random pairings of the IMF (dashed). We fit a power-law distribution with an intermediate slope of $\gamma = -1.2 \pm 0.4$ across $q = 0.1$–1.0 (blue). The data are also consistent with the segmented power-law model adopted in Moe & Di Stefano (2017; green). In total, we find that $57\% \pm 12\%$ of Cepheids have companions across $q = 0.1$–1.0 and $a = 1$–1000 au.

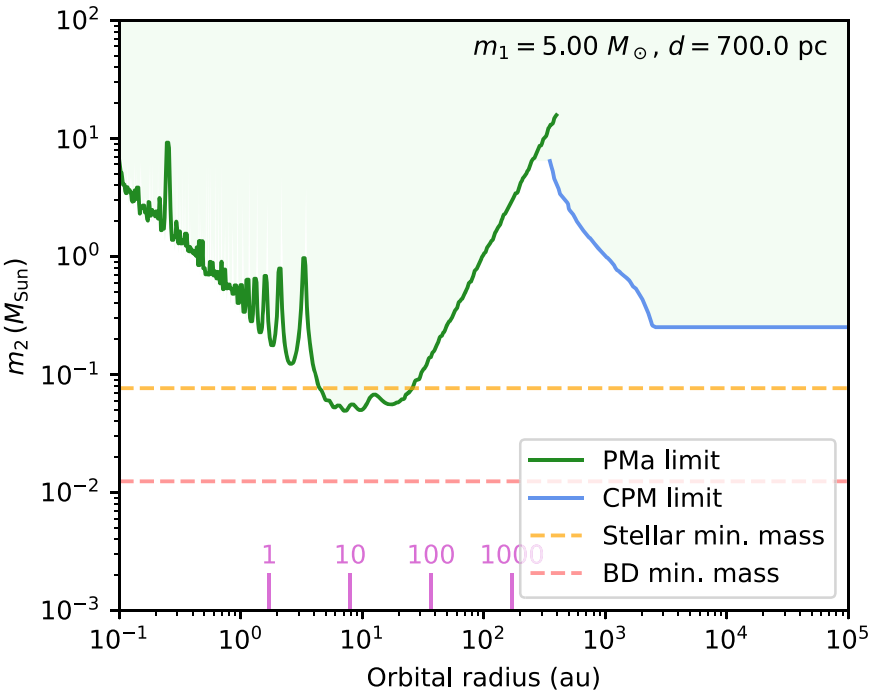

Figure 6. Companion detection sensitivity for Cepheids from Gaia EDR3. Sensitivity for companion mass is shown as a function of orbital radius and orbital period. Green line: limit from proper-motion anomaly; blue line: limit for common proper motions; yellow dashed line: stellar mass limit; pink dashed line: brown dwarf limit; orbital period in years is shown by the pink lines on the x-axis. Cepheid parameters are 5.0 $M_\odot$ and 700 pc, typical parameters in this study. The green region above the stellar limit indicates that stellar companions at the low-mass stellar limit will be detected for orbital periods between about 3 and 100 yr.

can exist around a massive star (Janson et al. 2021), providing the need to hunt for even smaller objects. Observing a sample of M stars to explore the mass distribution would require very long exposures in X-rays. Kervella et al. (2022) discuss the use of Gaia EDR3 proper motions and parallaxes to identify companions around stars within 100 pc through proper-motion anomalies (PMa orbital motion) and common proper-motion pairs (CPM). This sample includes relatively few massive stars; however, they find that 45% of the sample members have an indication of binarity and 7% have bound CPM candidates. They estimate that as many as 70% of Cepheid-mass stars could have PMa and CPM companions. Figure 6 shows the

detection limits for a typical Cepheid in this study ($5\,M_{\odot}$ and 700 pc) in EDR3. Stars down to the low-mass limit should be detected for orbital periods between about 3 and 100 yr. This limit will improve substantially in future Gaia releases, to approximately 4× better in DR4 (2024) and 13× better in DR5 (2027).

7. Summary

In this section we summarize the main points of this study.

7.1. l Car and Polaris

As shown in Figure 3, *l* Car has an X-ray luminosity that is below the quiescent phases of δ Cep, and certainly below the X-ray burst at maximum radius in δ Cep. Because *l* Car has a longer period than δ Cep, we know that it has a higher luminosity and mass, as well as reaching cooler minimum temperatures. Any of these could affect X-ray production, though it is not obvious that they would affect the convective surface to disrupt magnetic activity. While the observation was carefully timed for maximum radius, in a 35-day Cepheid, the 80 ks exposure covers only 3% of the phase, so a phase-restricted burst could have been missed.

For Polaris, the X-ray luminosity is comparable to that of δ Cep in its quiescent phases. There is no indication of an X-ray burst even though much of the pulsation cycle has been covered. The observation discussed here alone covers a phase range of 0.48−0.69. Polaris pulsates in the first-overtone mode and has a very low pulsation amplitude, which could alter the X-ray–pulsation relation as compared with δ Cep (full amplitude and fundamental mode).

7.2. The Pulsation Cycle

A major motivation for the series of X-ray observations of Cepheids follows from the X-ray burst in δ Cep. Figure 3 shows that neither η Aql nor *l* Car shares this behavior. As discussed above, *l* Car differs from δ Cep in physical properties that might account for this. η Aql, on the other hand, has a period very similar to δ Cep, and hence similar luminosity, mass, and temperature cycle. At this point, questions remain about the X-ray behavior of both stars. Polaris has no indication of a phase-related X-ray increase.

7.3. Low-mass Companions

Chandra and XMM-Newton observations of a sample of 20 Cepheids find that 28% have a low-mass companion. The fraction of Cepheids with low-mass companions is very similar to that predicted from mid-B stars. This sample identifying F, G, and K spectral type companions can be combined with a previous survey in the UV that identifies B and early A companions. Using a Moe and Di Stefano segmented power law to fit the data, $57\% \pm 12\%$ have companions with mass ratio $q > 0.1$ and separation $a > 1$ au. This is the first survey of intermediate-mass stars that reaches to mass ratios this small. The mass ratio distribution falls between a uniform distribution and random pairings from IMF, that is, between formation from shared accretion in a circumbinary disk and fragmentation and independently accreted components.

This research is based on observations obtained with XMM-Newton, an ESA science mission with instruments and contributions directly funded by ESA Member States and the USA (NASA).

Support was provided to NRE by the Chandra X-ray Center NASA contract NAS8-03060. The observations were associated with program 84051, with support for this work from NASA grant 80NSSC20K0794. J.J.D. was supported by NASA contract NAS8-03060 to the Chandra X-ray Center and thanks the director, Pat Slane, for continuing advice and support. H.M.G. was supported through grant HST-GO-15861.005-A from the STScI under NASA contract NAS5-26555. P.K. and L.B. acknowledge funding from the European Research Council (ERC) under the European Union's Horizon 2020 research and innovation program (projects CepBin, grant agreement No. 695099, and UniverScale, grant agreement No. 951549). This work has made use of data from the European Space Agency (ESA) mission Gaia (http://www.cosmos.esa.int/gaia), processed by the Gaia Data Processing and Analysis Consortium (DPAC, http://www.cosmos.esa.int/web/gaia/dpac/consortium). Funding for the DPAC has been provided by national institutions, in particular the institutions participating in the Gaia Multilateral Agreement.

The SIMBAD database and NASA's Astrophysics Data System Bibliographic Services were used in the preparation of this paper.

ORCID iDs

Nancy Remage Evans https://orcid.org/0000-0002-4374-075X
Scott Engle https://orcid.org/0000-0001-9296-3477
Ignazio Pillitteri https://orcid.org/0000-0003-4948-6550
Edward Guinan https://orcid.org/0000-0002-4263-2650
H. Moritz Günther https://orcid.org/0000-0003-4243-2840
Scott Wolk https://orcid.org/0000-0002-0826-9261
Hilding Neilson https://orcid.org/0000-0002-7322-7236
Massimo Marengo https://orcid.org/0000-0001-9910-9230
Sofia Moschou https://orcid.org/0000-0002-2470-2109
Jeremy J. Drake https://orcid.org/0000-0002-0210-2276
Elaine M. Winston https://orcid.org/0000-0001-9065-6633
Pierre Kervella https://orcid.org/0000-0003-0626-1749
Louise Breuval https://orcid.org/0000-0003-3889-7709

References

Abt, H. A., Gomez, A. E., & Levy, S. G. 1990, ApJS, 74, 551
Anderson, R. I. 2016, MNRAS, 463, 1707
Anderson, R. I. 2019, A&A, 623, A146
Anderson, R. I., Mérand, A., Kervella, P., et al. 2016, MNRAS, 455, 4231
Anderson, R. I., Sahlmann, J., Holl, B., et al. 2015, ApJ, 804, 144
Ayres, T. 2011, ApJ, 738, 120
Banyard, G., Sana, H., Mahy, L., et al. 2022, A&A, 658, 69
Benedict, G. F., McArthur, B. E., Feast, M., et al. 2007, AJ, 133, 1810
Berdnikov, L. N., Dambis, A. K., & Vozyakova, O. V. 2000, A&AS, 143, 211
Berghoefer, T. W., Schmitt, J. H. M. M., Danner, R., & Cassinelli, J. P. 1997, A&A, 322, 167
Bono, G., Marconi, M., Cassisi, S., et al. 2005, ApJ, 621, 966
Breuval, L. 2021, PhD Thesis, Univ. Paris
Chabrier, G. 2003, PASP, 115, 763
Drilling, J. S., & Landolt, A. U. 2000, in Astrophysical Quantities, ed. A. N. Cox (New York: Springer), 381
Engle, S. G. 2015, PhD Thesis, James Cook Univ.
Engle, S. G., Guinan, E. F., Harper, G. M., et al. 2017, ApJ, 838, 67
Evans, N. R. 1992, ApJ, 384, 220
Evans, N. R., Berdnikov, L., Lauer, J., et al. 2015, AJ, 150, 13
Evans, N. R., Bond, H. E., Schaefer, G. H., et al. 2013, AJ, 146, 93
Evans, N. R., Bond, H. E., Schaefer, G. H., et al. 2016a, AJ, 151, 129
Evans, N. R., DeGoia-Eastwood, K., Gagné, M., et al. 2011, ApJS, 194, 13
Evans, N. R., Guenther, H. M., Bond, H. E., et al. 2020b, ApJ, 905, 81

Evans, N. R., Karovska, M., Bond, H. E., et al. 2018, ApJ, 863, 187
Evans, N. R., Massa, D., & Proffitt, C. 2009, AJ, 137, 3700
Evans, N. R., Pillitteri, I., Kervella, P., et al. 2021, AJ, 162, 92
Evans, N. R., Pillitteri, I., & Molnar,, L. 2020a, AJ, 159, 121
Evans, N. R., Pillitteri, I., Wolk, S., et al. 2016b, AJ, 151, 108
Fernie, J. D., Evans, N. R., Beattie, B., & Seager, S. 1995, IBVS, 4148, 1
Gallenne, A., M'erand, A., Kervella, P., et al. 2016, MNRAS, 461, 1451
Gallenne, A., M'erand, A., Kervella, P., et al. 2021, A&A, 651, A113
Gullikson, K., Kraus, A., & Dodson-Robinson, S. 2016, AJ, 152, 40
Hocdé, V., Nardetto, N., Borgniet, S., et al. 2020b, A&A, 641, A74
Hocdé, V., Nardetto, N., Lagadec, E., et al. 2020a, A&A, 633, A47
Hocdé, V., Nardetto, N., Matter, A., et al. 2021, A&A, 651, A92
Janson, M., Gratton, R., Roder, L., et al. 2021, Natur, 600, 231
Kervella, P., Arenou, F., & Thévenin, F. 2022, A&A, 657, 7
Kervella, P., Gallenne, A., Evans, N. R., et al. 2019a, A&A, 623, A116
Kervella, P., Gallenne, A., Evans, N. R., et al. 2019b, A&A, 623, A117
Kobulnicky, H. A., & Fryer, C. L. 2007, ApJ, 670, 747
Kouwenhoven, M. B. N., Brown, A. G. A., Portegies Zwart, S. F., & Kaper, L. 2007, A&A, 474, 77
Merand, A., Kervella, P., Coude du Foresto, V., et al. 2006, A&A, 453, 155
Meynet, G., Mermilliod, J.-C., & Maeder, A. 1993, A&AS, 98, 477
Moe, M., & Di Stefano, R. 2017, ApJS, 230, 15
Naze, Y., Broos, P., Oskinova, L., et al. 2011, ApJS, 215, 10
Neilson, H. R., Engle, S. G., Guinan, E. F., Bisol, A. C., & Butterworth, N. 2016, ApJ, 824, 1
Pillitteri, I., Evans, N. R., Wolk, S., & Syal, M. B. 2013, AJ, 145, 143
Prebisch, T., & Feigelson, E. D. 2005, ApJS, 160, 390
Randich, S., Schmitt, J. H. M. M., Prosser, C. F., & Stauffer, J. R. 1996, A&A, 305, 785
Rizzuto, A. C., Ireland, M. J., Robertson, J. G., et al. 2013, MNRAS, 436, 1694
Sana, H., de Mink, S. E., de Koter, A., et al. 2012, Sci, 337, 444
Seward, F. D. 2000, in Astrophysical Quantities, ed. A. N. Cox (New York: Springer), 381
Stauffer, J. R., Barrado y Navascues, D., Bouvier, J., et al. 1999, ApJ, 527, 219
Szabados, L. 1989, Mitt. Sternwarte Ungar Akad Wissen, 94, 1
Szabados, L. 1991, Mitt. Sternwarte Ungar Akad Wissen, 96, 123
Taylor, M. M., Albrow, M. D., Booth, A. J., & Cottrell, P. L. 1997, MNRAS, 292, 662
Usenko, I. A., Kniazev, A. Yu., Berdnikov, L. N., Fokin, A. B., & Kravtsov, V. V. 2014, AstL, 40, 435
Usenko, I. A., Kniazev, A. Yu., Berdnikov, L. N., Kravtsov, V. V., & Fokin, A. B. 2013, AstL, 39, 432